ACS Catalysis

Letter

pubs.acs.org/acscatalysis

Multifunctional Au−Co@CN Nanocatalyst for Highly Efficient Hydrolysis of Ammonia Borane

Lin-Tong Guo, Yi-Yu Cai, Jie-Min Ge, Ya-Nan Zhang, Ling-Hong Gong, Xin-Hao Li,* Kai-Xue Wang, Qi-Zhi Ren,* Juan Su, and Jie-Sheng Chen

School of Chemistry and Chemical Engineering, Shanghai Jiao Tong University, Shanghai 200240, P. R. China

Supporting Information

ABSTRACT: A magnetically recyclable carbon nitride supported Au−Co nanoparticles (Au−Co@CN) displayed exceedingly high photocatalytic activity for hydrolysis of aqueous ammonia borane (NH_3BH_3, AB) solution. Combined with a synergetic effect between Au and Co nanoparticles, the Motty−Schottky effect at the metal−semiconductor interface remarkably facilitated the catalytic performance of the Au−Co@CN catalyst on the hydrolysis of AB. The TOF value of Au−Co@CN catalyst is 2897 mol H_2 mol^{-1} metal h^{-1} at 298 K under visible light irradiation, which is more than 3 times higher than that of the benchmarked catalyst, PVP-stabilized Au@Co nanoparticles.

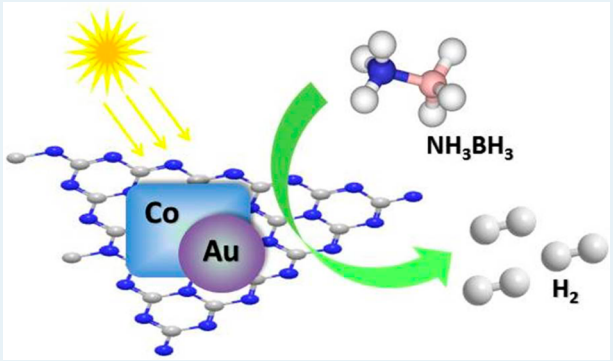

KEYWORDS: *ammonia borane, carbon nitride, Au−Co nanoparticles, hydrolysis, magnetically recyclable, photocatalysis*

The increasing requirement of clean energy sources without carbon-based emissions and other pollutants has resulted in increased attention to the "hydrogen economy", the key point of which is to find a safe and efficient storage medium.[1−3] Ammonia borane (NH_3BH_3, AB) has emerged as one of the leading candidates for hydrogen storage materials due to its relatively high hydrogen storage capacity (19.6 wt % of H_2).[4−7] Thus, sustainable, cheap and efficient catalysts are poorly needed to release hydrogen gas from AB under mild condition for practical applications. Dehydrogenation of AB can be catalyzed over homogeneous metal complexes by adding base and/or organic ligands to get high hydrogen generation rates.[6−9] It is obvious that the difficulty in separating those homogeneous catalysts from the solvents makes them inconvenient for multiple uses in large scale. Alternatively, heterogeneous catalysts involving metal nanoparticles can be reused, though less active than the homogeneous counterparts. The ideal sustainable catalysts should be recyclable, cheap, and efficient for dehydrogenation of AB in green solvents without any other additives at room temperature.

In the past, noble metal nanoparticle-based catalysts became the mainstream of heterogeneous catalysts for the hydrolysis of AB, but the price of the expensive catalysts rather obstructed their practical applications.[10−12] Bimetallic NPs with non-noble metal contents have attracted considerable research interest in recent years due to their unique optical, electrical, magnetic, and catalytic properties compared with the monometallic counterparts, such as Au−Co, Au−Fe, Ru−Co, Fe−Pt etc.[13−17] More importantly, the introduction of certain amount of non-noble metal components could significantly reduce the cost of these catalysts without sacrificing the catalytic activity. Rationally engineering the nanostructure of these bimetallic nanoparticles to form homogeneous alloy or core−shell structures has been applied to further elevate their final catalytic performance. However, their complicated fabrication processes with harsh reaction conditions and the use of expensive additives contradict the conception of green chemistry. Approaches for significantly enhancing the activity of bimetallic nanoparticle-based heterogeneous catalysts for dehydrogenation of AB under mild conditions without sacrificial additives are still challenging.

Support effects can be utilized for restraining the agglomeration of the metal NPs and improving their dispersion over the surface of catalyst support.[18] Typical catalyst supports, including metal oxides,[19] activated carbons,[10,20,21] and metal−organic frameworks,[22−24] have been adopted to stabilize NPs and obtain more effective heterogeneous catalysts for dehydrogenation of AB. After effectively resolving the stability issues, more efforts are moving toward the study of the synergistic effect between the metal nanoparticles and catalyst support. Among the supports available for the embedding of metal NPs, nanostructured carbon nitride (g-C_3N_4, also abbreviated as CN) with a band gap of around 2.7 eV has proved to be an ideal candidate, because the work functions of most metals are located between the conduction band and the valence band of g-C_3N_4.[25−28] The organic moieties of g-C_3N_4 could also help to stabilize NPs for more effective

Received: June 13, 2014
Published: December 10, 2014

heterogeneous catalysts.[29] Recently, there has been some attempts to investigate the possibility of applying the Mott−Schottky catalysis to enhance the catalytic performance of metal nanoparticles for water splitting, artificial photosynthesis, and other catalytic reactions.[26−35] A rectifying contact between the metal NPs and the semiconductive support is required to obtain effective Mott−Schottky catalysts, resulting in the electron transfer to the metal side with higher "nobility" (Figure 1). Rational design of Schottky heterojunction between

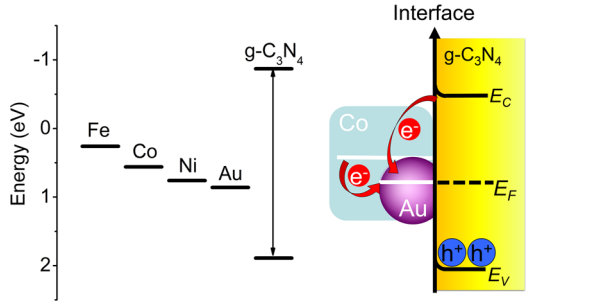

Figure 1. (a) Work functions of typical metals and band structures of carbon nitride. (b) Schematic view of Mott−Schottky type contact based on Au−Co hybrid nanoparticles.

the semiconductive support and metal nanoparticles combined with the high activity of bimetallic nanoparticles may principally elevate the catalytic performance of the hybrid nanocatalyst to a great extent.

In order to improve the diffusion aspect of the dehydrogenation reaction of solid AB, solvents are usually required to ensure the high output of hydrogen gas for practical use. Consequently, such a process results in the impeding of the fast separation of catalysts from solution after use. Herein, we described the fabrication of multifunctional carbon nitride supported Au−Co bimetallic nanoparticles (Au−Co@CN) for highly efficient, room-temperature dehydrogenation of aqueous AB under ambient atmosphere. Besides the very high activity, the resultant Au−Co@CN materials are magnetical and can be recycled fast and facilely by using an external magnetic bar.[15] Au−Co@CN can also act as a photocatalyst to give a much higher reaction rate under visible light irradiation.

The mesoporous carbon nitride with a surface area of 160 m^2/g and the pore size distribution centered at 14 nm was chosen as the organic semiconductor catalyst support since it has the suitable band position for constructing rectifying contact (Figure 1b and S1 in Supporting Information (SI)). As shown in Figure 1a, the work functions of many metals like Fe, Co, Ni, and Au lie between the conduction band and the valence band of carbon nitride, suitable for constructing a rectifying Mott−Schottky heterojunction. The first-row transition metals, including Fe, Co, and Ni, were selected as potential cocatalysts due to their low cost and high abundance in nature. More importantly, recent theoretical and experimental results also showed that either bare Fe, Co, or Ni nanoparticles or their multicomponent nanohybrids can offer good to excellent catalytic activities for various hydrogen evolution reactions including dehydrogenation of AB.[1−10,15−17,20,21,36−38]

Multifunctional Au−Fe@CN, Au−Co@CN and Au−Ni@CN catalysts were prepared via a modified wet impregnation method (for detailed method, see SI). Further characterization was conducted for Au−Co@CN as the typical sample. This is because Au−Co@CN offered the best catalytic performance for dehydrogenation of AB with an optimized molar ratio of 4:96 (Au/Co) here (Figure S2), matching well with the results of unsupported Au−Co nanoparticles.[15] Molecular stabilizers were not employed in the synthetic process to avoid the formation of possible insulating layer between metal and carbon nitride.

The successful deposition of metallic Au and Co on the surface of carbon nitride support was confirmed by the powder X-ray diffraction (PXRD) and nitrogen sorption analysis, and the transmission electron microscopy (TEM) observation. As indicated by the TEM images of typical Au−Co@CN sample (Figure S3), the sizes of the Au nanoparticles on carbon nitride were mainly smaller than 10 nm, similar to the size of Au NPs deposited inside ordered mesoporous carbon nitride materials.[29] Obviously, the carbon nitride support could stabilize as-formed Au nanoparticles due to its amine-rich surface. As the major components of the bimetallic nanoparticles, the Co nanoparticles (96 at. % of the total metal content) are roughly in the amorphous phase, as demonstrated by the weak and broad XRD peaks (Figure S4), whereas the XRD peaks of the Au NPs (4 at. % of the total metal content) are much stronger. High-resolution TEM images of the sample (Figure S3b) further confirmed the formation of Au nanocrystals and larger Co amorphous nanoparticles with irregular shape and a size ranged from several to tens of nanometers. The nitrogen adsorption analysis results (Figure S1) suggest that the nanopores of mesoporous carbon nitride were partially filled with metal components, resulting in smaller surface area (93 m^2/g), pore volume, and pore size. Such a hybrid Au−Co nanostructure with Au core completely or partly covered by Co shells may benefit their potential applications in catalysis. Indeed, it is the tandem reduction of Au and Co by using AB as a mild reductant that led to the formation of such a unique hybrid nanostructure.[15] No obvious change in the FTIR spectra of the samples after the metal loading was observed, presenting well the chemical stability of the carbon nitride support (Figure S5).

Catalytic tests on hydrolysis of aqueous AB were carried out at room temperature, which is an ideally mild condition for practical usage. The support effect of carbon nitride is clearly demonstrated in the study of catalytic hydrogenation generation. As shown in Figure 2a, Au−Co@CN (30 wt %, if not otherwise specified) completed the decomposition of AB within 5 min, which is much faster than that of the unsupported sample Au−Co (10 min). Visible light ($\lambda \geq 400$ nm) further boosts the catalytic activity of Au−Co@CN, shortening the decomposition process to 150 s. Although previous reports about the effect of the conducting carbon support such as graphene and the insulating metal oxides supports focus mainly on the increased dispersion of metal nanoparticles, our results suggest that the variation of the electron structure of metals when coupled with the semiconductor supports could achieve a remarkable improvements of the activity.

The elevated catalytic property of supported Au−Co@CN is attributed to the electron enrichment of metal nanoparticles, which is named the Mott−Schottky effect. Driven by the difference of the work function, the electron flows from the conduction band of carbon nitride to the metal side, forming a potential barrier. No backward flow is allowed after this Schottky barrier is built. Under visible light irradiation, the excitation of carbon nitride injects more electrons to the metal nanoparticles and obtained enhanced charge separation. This

dx.doi.org/10.1021/cs501692n | ACS Catal. 2015, 5, 388−392

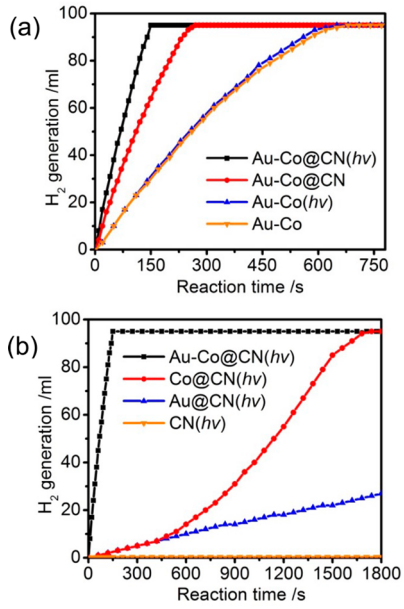

Figure 2. (a) Hydrolysis of aqueous AB solution catalyzed by Au−Co@CN or Au−Co with or without photoirradiation ($\lambda \geq 400$ nm). (b) Hydrolysis of aqueous AB solution catalyzed by Au−Co@CN, Co@CN and Au@CN with photoirradiation ($\lambda \geq 400$ nm). Typical conditions: 0.26 M aqueous AB solution (5 mL), molar ratio of catalyst/AB = 0.02, ambient atmosphere = 298 K.

was revealed by the distinct decrease of the photoluminescence of carbon nitride after metal loading (Figure S6) while the band gap was not changed obviously after the deposition of metal nanoparticles as estimated by the similar absorption edge of the samples (Figure S7). It seems that the electron enrichment caused by illumination further improved the catalytic performance of Au−Co@CN. Besides the electron injection from CN to metal, surface plasmonic effect was also another possibility for enhancing the photocatalytic activity, while plasma absorption of Au NPs was also observed in the UV−vis adsorption spectra of Au−Co@CN (Figure S7). The fact that the activity of unsupported catalyst Au−Co offered similar hydrogen evolution rates (Figure 2a) for both dark and photocatalytic reactions, excludes the possible influence of thermal effect or surface plasmonic effect on the catalysis process here. The Mott−Schottky effect, as demonstrated in our previous reports for organic synthesis and decomposition of formic acid,[31−34] also plays a key role in facilitating the rate of hydrolysis reaction of AB here (Scheme S1).[36]

The synergetic effect between Au and Co nanoparticles also plays a critical role in enhancing the photocatalytic performance of Au−Co@CN. Co@CN and Au@CN shows relatively poor activity compared with Au−Co@CN (Figure 2b). To find the origin of the synergetic effect, further analysis on the structure of the metal NPs were conducted. Generally, an Au−Co interface, as has been demonstrated by the HRTEM observation (Figure S3b), is believed to be the most active cites in the metal nanoparticles. As shown by Xu et al., the control of the stepwise reduction process by rationally selecting reductant is of key importance to construct such a kind of bimetallic interface.[15] Homogeneous metal alloy obtained by fast reduction using $NaBH_4$ could only offer a moderate catalytic activity.

The metal loading proportion was then optimized by evaluating the catalytic activity of Au−Co@CN with the metal weight percentages range from 1.5 wt % to 90 wt %. The atomic ratio of Au and Co was optimized to be 4:96 for all samples. The rates of hydrogen generation gradually increased with more metal loadings up to the optimum value of 30 wt % (Figure 3a and Figure S8). However, too much metal deposited

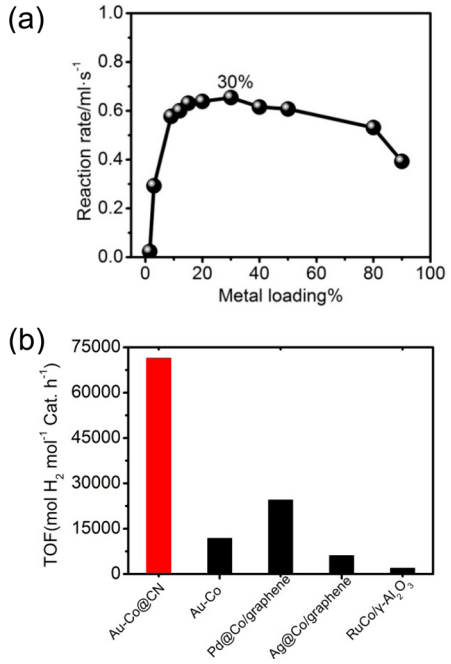

Figure 3. (a) Hydrogen generation from aqueous AB solution catalyzed by Au−Co@CN-x% (x%: weight percentages of metal contents, x = 1.5−90) under photoirradiation. (b) TOF values for hydrogen evolution via decomposition of AB over Au−Co@CN described in this work and various benchmarked catalysts in the literature: Au@Co,[15] Pd@Co/graphene,[37] RuCo/γ-Al_2O_3[38] and Ag@Co/graphene.[21] The amounts of catalyst (Cat.) were calculated on the basis of the moles of noble metal components involved.

on the surface of CN will potentially impede the light-harvesting process as well as the approach of the reactant to the as-formed active site located at the interface of metal and support. This is because the available sites for building the effective metal−semiconductor contact are limited on the surface of CN. As a result, further increase in the metal loading from 30 wt % to 90 wt % could only lead to ever worse catalytic activities of the catalysts.

After optimizing the various catalytic parameters for the dehydrogenation of AB, the best catalyst Au−Co@CN with a metal loading of 30 wt % and an atomic ratio of 4:96 (Au/Co) achieved a remarkable TOF value of 1704 mol H_2 mol^{-1} metal h^{-1}, which is about twice of that over PVP-stabilized Au@Co nanoparticles.[15] Visible light irradiation could further improve the TOF value of Au−Co@CN to 2897 mol H_2 mol^{-1} metal h^{-1}. This TOF value is significantly higher than those over reported Au and/or Co NPs based catalysts reported in the literature (Figure 3b and Table S1).[15−17,20,21,37,38] It is worth noting that TOF of our catalyst was as high as 71410 mol H_2 mol^{-1} noble metal h^{-1}, surpassing that (24540 mol H_2 mol^{-1} noble metal h^{-1}) of the benchmarked catalyst Pd@Co/graphene in the literature.[37] It is thus obvious that such a photocatalytic responsibility of Au−Co@CN combined with the synergetic effect between Au and Co nanoparticles is highly efficient for dehydrongenaion of AB for hydrogen evolution

dx.doi.org/10.1021/cs501692n | ACS Catal. 2015, 5, 388−392

reaction, promising great potential to rationally construct useful metal−semiconductor interface and also bimetallic or trimetallic interfaces for further facilitating the final catalytic activity to a great extent (Scheme S1).

As important issues for practical use of heterogeneous catalyst, both the stability and the reusability should be tested. The supraparamagnetic Au−Co NPs (Figure S9) in the catalyst bring the advantage of easy separation using an external magnet,[39,40] which greatly facilitate the recycle process of the catalyst (Figure 4b). The recycling experiment of Au−Co@CN

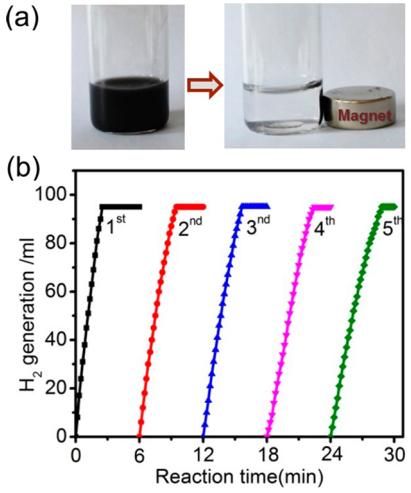

Figure 4. (a) Photographs of the Au−Co@CN dispersions before and after magnetic separation. (b) Hydrolysis of aqueous AB solution catalyzed by Au−Co@CN from the 1st to 5th cycle under photoirradiation. Typical conditions were described in Figure 2. The reaction vessel was refilled with fresh aqueous AB solution every 6 min after the magnetic separation of Au−Co@CN.

was conducted facially by a magnetic separation procedure (Figure 4a) and then replenishing the reaction vessel with fresh aqueous AB solution every 6 min. As shown in Figure 4b, there was only a slight decrease in catalytic activity even after five rounds of reactions, indicating a well-established reusability for practical applications. The chemical stability of carbon nitride support was also high as revealed by the FTIR spectra of the used sample (Figure S5). Again, the strong interaction between Au−Co NPs and CN afforded the hybrid catalyst superb stability.

In conclusion, we highlighted the construction of multifunctional Au−Co@CN hybrid nanocatalyst for highly efficient dehydrogenation of aqueous AB solution in this work. Under mild conditions, Au−Co@CN displayed exceedingly high photocatalytic activity for hydrogen generation, surpassing the benchmarked catalysts reported previously. The synergetic effect between Au and Co nanoparticles and the Mott−Schottky effect at the metal−carbon nitride interface were proved to account for the outstanding catalytic propriety of Au−Co@CN. Also, the simple and cost-effective fabrication process, the magnetic recyclability, and the good stability of Au−Co@CN paves its way for practical applications. Also, the ambient sun rays can be chosen as light source to significantly accelerate the hydrogen generation rate without adding organic ligands or more Au nanoparticles. That way, the cost for corresponding applications will be reduced largely. Further extending the application of Mott−Schottky effect and bimetallic synergetic effect to fabrication of efficient nanocatalysts for both hydrogen storage and organic synthesis[41] will also be tried in our group.

■ ASSOCIATED CONTENT

Supporting Information

The following file is available free of charge on the ACS Publications website at DOI: 10.1021/cs501692n.

Synthesis and characterization (BET, TEM, PXRD) of catalysts, proposed reaction mechanism, TOF values (PDF)

■ AUTHOR INFORMATION

Corresponding Authors

*E-mail: (X.-H.L) xinhaoli@sjtu.edu.cn.

*E-mail: (Q.-Z.R.) qzren@sjtu.edu.cn.

Notes

The authors declare no competing financial interest.

■ ACKNOWLEDGMENTS

This work was financially supported by National Basic Research Program of China (2013CB934102, 2011CB808703) and the National Natural Science Foundation of China (21331004, 21301116).

■ REFERENCES

(1) Gutowska, A.; Li, L.; Shin, Y.; Wang, C. M.; Li, X. S.; Linehan, J. C.; Smith, R. S.; Kay, B. D.; Schmid, B.; Shaw, W.; Gutowski, M.; Autrey, T. *Angew. Chem., Int. Ed.* **2005**, *44*, 3578−3582.

(2) Denney, M. C.; Pons, V.; Hebden, T. J.; Heinekey, D. M.; Goldberg, K. I. *J. Am. Chem. Soc.* **2006**, *128*, 12048−12049.

(3) Himmelberger, D. W.; Yoon, C. W.; Bluhm, M. E.; Carroll, P. J.; Sneddon, L. G. *J. Am. Chem. Soc.* **2009**, *131*, 14101−14110.

(4) Stephens, F. H.; Pons, V.; Baker, R. T. *Dalton Trans.* **2007**, 2613−2626.

(5) Davis, B. L.; Dixon, D. A.; Garner, E. B.; Gordon, J. C.; Matus, M. H.; Scott, B.; Stephens, F. H. *Angew. Chem., Int. Ed.* **2009**, *48*, 6812−6816.

(6) Kim, S. K.; Han, W. S.; Kim, T. J.; Kim, T. Y.; Nam, S. W.; Mitoraj, M.; Piekoś, Ł.; Michalak, A.; Hwang, S. J.; Kang, S. O. *J. Am. Chem. Soc.* **2010**, *132*, 9954−9955.

(7) Metin, Ö.; Duman, S.; Dinç, M.; Özkar, S. *J. Phys. Chem. C* **2011**, *115*, 10736−10743.

(8) Fukuzumi, S.; Yamada, Y.; Suenobu, T.; Ohkubo, K.; Kotani, H. *Energy Environ. Sci.* **2011**, *4*, 2754−2766.

(9) Marziale, A. N.; Friedrich, A.; Klopsch, I.; Drees, M.; Celinski, V. R.; Günne, J. S.; Schneider, S. *J. Am. Chem. Soc.* **2013**, *135*, 13342−13355.

(10) Akbayrak, S.; Özkar, S. *ACS Appl. Mater. Interfaces* **2012**, *4*, 6302−6310.

(11) Chandra, M.; Xu, Q. *J. Power Sources* **2007**, *168*, 135−142.

(12) Yadav, M.; Xu, Q. *Energy Environ. Sci.* **2012**, *5*, 9698−9725.

(13) Cui, Y.; Ren, B.; Yao, J. L.; Gu, R. A.; Tian, Z. Q. *J. Phys. Chem. B* **2006**, *110*, 4002−4006.

(14) Lee, Y. W.; Kim, M.; Kim, Z. H.; Han, S. W. *J. Am. Chem. Soc.* **2009**, *131*, 17036−17037.

(15) Yan, J. M.; Zhang, X. B.; Akita, T.; Haruta, M.; Xu, Q. *J. Am. Chem. Soc.* **2010**, *132*, 5326−5327.

(16) Cao, N.; Su, J.; Luo, W.; Cheng, G. Z. *Catal. Commun.* **2014**, *43*, 47−51.

(17) Li, J.; Zhu, Q. L.; Xu, Q. *Chem. Commun.* **2014**, *50*, 5899−5901.

(18) Wan, Y.; Wang, H. Y.; Zhao, Q. F.; Klingstedt, M.; Terasaki, O.; Zhao, D. Y. *J. Am. Chem. Soc.* **2009**, *131*, 4541−4550.

(19) Kaya, M.; Zahmakiran, M.; Özkar, S.; Volkan, M. *ACS Appl. Mater. Interfaces* **2012**, *4*, 3866−3873.

(20) Qiu, F. Y.; Li, L.; Liu, G.; Wang, Y. J.; An, C. H.; Xu, C. C.; Xu, Y. N.; Wang, Y.; Jiao, L. F.; Yuan, H. T. *Int. J. Hydrogen Energy* **2013**, *38*, 7291−7297.
(21) Yang, L.; Luo, W.; Cheng, G. Z. *ACS Appl. Mater. Interfaces* **2013**, *5*, 8231−8240.
(22) Jiang, H. L.; Akita, T.; Ishida, T.; Haruta, M.; Xu, Q. *J. Am. Chem. Soc.* **2011**, *133*, 1304−1306.
(23) Aijaz, A.; Karkamkar, A.; Choi, Y. J.; Tsumori, N.; Rönnebro, E.; Autrey, T.; Shioyama, H.; Xu, Q. *J. Am. Chem. Soc.* **2012**, *134*, 13926−13929.
(24) Zhu, Q. L.; Li, J.; Xu, Q. *J. Am. Chem. Soc.* **2013**, *135*, 10210−10213.
(25) Vinu, A.; Ariga, K.; Mori, T.; Nakanishi, T.; Hishita, S.; Golberg, D.; Bando, Y. *Adv. Mater.* **2005**, *17*, 1648−1652.
(26) Talapaneni, S. N.; Anandan, S.; Mane, G. P.; Anand, C.; Dhawale, D. S.; Varghese, S.; Mano, A.; Mori, T.; Vinu, A. *J. Mater. Chem.* **2012**, *22*, 9831−9840.
(27) Mane, G. P.; Dhawale, D. S.; Anand, C.; Ariga, K.; Ji, Q. M.; Wahab, M. A.; Mori, T.; Vinu, A. *J. Mater. Chem. A* **2013**, *1*, 2913−2920.
(28) Jia, L. C.; Wang, H. Q.; Dhawale, D.; Anand, C.; Wahab, M. A.; Ji, Q. M.; Ariga, K.; Vinu, A. *Chem. Commun.* **2014**, *50*, 5976−5979.
(29) Datta, K. K. R.; Reddy, B. V. S.; Ariga, K.; Vinu, A. *Angew. Chem., Int. Ed.* **2010**, *49*, 5961−5965.
(30) Wang, Y.; Yao, J.; Li, H. R.; Su, D. S.; Antonietti, M. *J. Am. Chem. Soc.* **2011**, *133*, 2362−2365.
(31) Cai, Y. Y.; Li, X. H.; Zhang, Y. N.; Wei, X.; Wang, K. X.; Chen, J. S. *Angew. Chem., Int. Ed.* **2013**, *52*, 11822−11825.
(32) Li, X. H.; Antonietti, M. *Chem. Soc. Rev.* **2013**, *42*, 6593−6604.
(33) Li, X. H.; Wang, X. C.; Antonietti, M. *Chem. Sci.* **2012**, *3*, 2170−2174.
(34) Li, X. H.; Baar, M.; Blechert, S.; Antonietti, M. *Sci. Rep.* **2013**, *3*, 1743(1−6).
(35) Li, X. H.; Chen, J. S.; Wang, X. C.; Sun, J. H.; Antonietti, M. *J. Am. Chem. Soc.* **2011**, *133*, 8074−8077.
(36) Talapaneni, S. N.; Mane, G. P.; Mano, A.; Anand, C.; Dhawale, D. S.; Mori, T.; Vinu, A. *ChemSusChem* **2012**, *5*, 700−708.
(37) Wang, J.; Qin, Y. L.; Liu, X.; Zhang, X. B. *J. Mater. Chem.* **2012**, *22*, 12468−12470.
(38) Rachiero, G. P.; Demirci, U. B.; Miele, P. *Int. J. Hydrogen Energy* **2011**, *36*, 7051−7065.
(39) Li, X. H.; Zhang, D. H.; Chen, J. S. *J. Am. Chem. Soc.* **2006**, *128*, 8382−8383.
(40) Wei, X.; Su, J.; Li, X. H.; Chen, J. S. *Dalton Trans.* **2014**, *43*, 16173−16177.
(41) Gong, L. H.; Cai, Y. Y.; Li, X. H.; Zhang, Y. N.; Su, J.; Chen, J. S. *Green. Chem.* **2014**, *16*, 3746−3751.